

Lazy-DaSH: Lazy Approach for Hypergraph-based Multi-robot Task and Motion Planning

Seongwon Lee¹, James Motes¹, Isaac Ngui¹, Marco Morales^{1,2}, and Nancy M. Amato¹

Abstract—We introduce Lazy-DaSH, an improvement over the recent state of the art multi-robot task and motion planning method DaSH, which scales to more than double the number of robots and objects compared to the original method and achieves an order of magnitude faster planning time when applied to a multi-manipulator object rearrangement problem. We achieve this improvement through a hierarchical approach, where a high-level task planning layer identifies planning spaces required for task completion, and motion feasibility is validated lazily only within these spaces. In contrast, DaSH precomputes the motion feasibility of all possible actions, resulting in higher costs for constructing state space representations. Lazy-DaSH maintains efficient query performance by utilizing a constraint feedback mechanism within its hierarchical structure, ensuring that motion feasibility is effectively conveyed to the query process. By maintaining smaller state space representations, our method significantly reduces both representation construction time and query time. We evaluate Lazy-DaSH in four distinct scenarios, demonstrating its scalability to increasing numbers of robots and objects, as well as its adaptability in resolving conflicts through the constraint feedback mechanism.

I. INTRODUCTION

Multi-robot systems are used in domains such as warehouse operations and assembly, enabling faster completion through parallel operations and achieving more complex tasks through coordination. Planning for such applications is challenging as the size of the planning space grows exponentially as both the number of robots and tasks increases and as the level of coordination required increases [1]. When the coordination required is low, decoupled multi-robot motion planning (MRMP) addresses this complexity by decomposing the search space into independent robot state spaces and later resolves conflicts between individual robot plans. However, multi-robot task and motion planning (MR-TMP) problems that require high levels of coordination are traditionally solved with coupled methods that directly consider the composite space of the system. This enables the necessary coordination but suffers from the exponential scaling of the search space. Recent work has explored hybrid approaches that aim to balance the strengths of coupled and decoupled approaches while minimizing their weaknesses.

In our prior work, we presented the **Decomposable State Space Hypergraph** (DaSH) framework [2], a hybrid approach for MR-TMP which seeks to focus computation effort only where coordination is needed through a more efficient

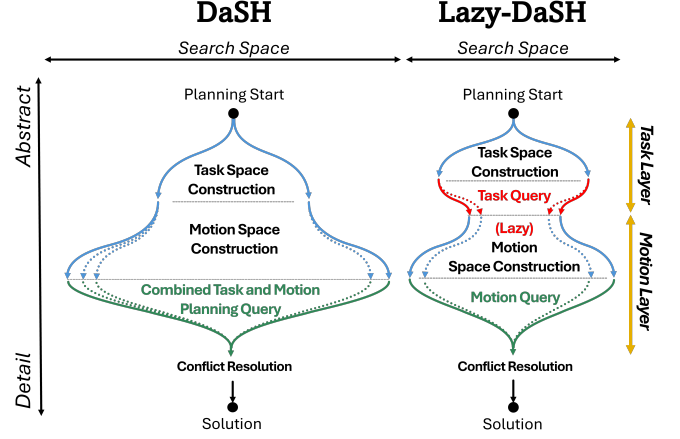


Fig. 1: A comparison of the search space scope during the search processes of DaSH and Lazy-DaSH. The introduction of the task query phase and lazy motion validation distinguishes our approach from DaSH, as highlighted in red. The task query narrows the search space, while lazy motion validation considers only motions in the candidate plan, reducing the computational cost of motion space construction. While both DaSH and Lazy-DaSH iteratively update representations upon plan failure, Lazy-DaSH employs a constraint feedback mechanism within a hierarchical framework to effectively manage both task-level and motion-level constraints, as illustrated in Fig. 2 and Algorithm 1.

hypergraph-based representation of the task space than traditional graph-based composite methods and produces smaller search spaces when considering the motion feasibility for groups of coupled robots and tasks. The original DaSH framework computes the motion feasibility within each of these smaller search spaces and then uses this information within a joint task and motion planning query (Fig. 1). This leads to very fast query times, but the construction time required to compute representations can be excessive, as high levels of task and motion coordination are required with the growing number of robots and objects.

This paper presents Lazy-DaSH, which reduces overall computational effort by lazily computing motion feasibility only within the set of decoupled planning spaces required by the current task plan. This requires the computation of a task plan before considering motion feasibility, earlier in the process than the original DaSH framework. This can be understood as selectively scoping the potentially relevant search space during the high-level planning process to reduce the computational effort required for the subsequent representation construction phase (Fig. 1). To further minimize computational overhead, motion planning is performed lazily, considering only the current task plan. If a required motion

¹Parasol Lab, University of Illinois Urbana-Champaign, USA {s1148, jmotest2, ingui2, moralesa, namato}@illinois.edu

² Department of Computer Science, Instituto Tecnológico Autónomo de México (ITAM), Mexico City, 01080, México. {marco.morales}@itam.mx.

is found to be infeasible, the task planning phase incorporates this information to generate a new task plan, leading to an alternative motion plan. This allows the planner to reduce the cost of expensive motion validation (e.g., collision checking) and focus on sequencing and identifying critical tasks and motions, calling motion validation only when necessary.

Our contribution can be summarized as a new MR-TMP algorithm, Lazy-DaSH, which features:

- A task planning layer into the DaSH hierarchy, featuring queryable task planning representation and task query strategy.
- Lazy motion validation of robot state spaces included in the task plan, with a task and motion constraint feedback mechanism for infeasible motions.
- Scalable and efficient replanning, scaling to twice the number of both robots and objects and achieving an order of magnitude faster planning times than DaSH in diverse multi-manipulator object rearrangement scenarios.

II. PRELIMINARIES AND RELATED WORK

In this section, we introduce the preliminaries and related work for MR-TMP.

A. Motion Planning

The position of a robot is completely parameterized by its degrees of freedom (DOF), which include its pose, orientation, and joint angles, and their values define a robot's configuration. The set of all robot configurations forms the *configuration space* (C_{space}). The motion planning problem seeks to find a continuous path between a start and goal configuration through the subset of valid configurations (C_{free}).

Representing the high-dimensional C_{space} explicitly is intractable in the general case [1]. To address this, sampling-based motion planning [3]–[8] randomly samples configurations in C_{space} to construct a graph or tree representation that approximates connectivity. Motion planning queries are answered by connecting the start and goal to this representation and computing a path over it.

B. Task and Motion Planning

When object manipulations are required, the robot needs to navigate and interact with these objects to achieve task objectives. This involves two layers: a task planning layer that determines the sequence of abstract actions and a motion planning layer that computes feasible motions to perform these actions. Integrating these layers allows robots to satisfy the constraints imposed by the robots and the environment. There are three major categories of approaches that focus on constraint satisfaction [9]: *sequencing-first*, *satisfaction-first*, and *interleaved approaches*.

Sequencing-first approaches plan high-level actions before determining the specific motions required to execute them [10]–[12]. They assume all actions have feasible motions during the high-level planning, which is frequently not the case due to physical constraints. Thus, they include mechanisms for backtracking and trying alternative plans when initial ones fail.

Satisfaction-first approaches focus on satisfying constraints related to continuous parameters (e.g., object positions and robot configurations) before creating an action sequence [13]–[15]. They are efficient when it is easier to sample and test these parameters upfront rather than repeatedly attempting to fit them into an action sequence that might not work. Thus, they often involve a cycle of sampling and testing for feasibility.

Interleaved approaches blend the sequencing of actions with the determination of parameter values, dynamically adapting both methods [16]–[19]. They enable a flexible and efficient planning process by minimizing unnecessary backtracking and reducing the computational overhead associated with either fully sequential or satisfaction-first methods.

C. Multi-robot Task and Motion Planning

Multi-robot task and motion planning extends the fundamental concepts of task and motion planning to complex tasks that require collaboration between multiple robots. This problem is significantly more complex when factoring in robot interactions in coordination, collision avoidance, and task allocation and scheduling [20].

Multi-manipulator object rearrangement is an important problem in MR-TMP requiring complex multi-robot coordination. The three classes of approaches—coupled, decoupled, and hybrid—are applicable in this context as well. Most MR-TMP problems require a high level of coordination, and the decoupled approach often fails to find a feasible solution. On the other hand, the coupled approach is capable of finding a highly coordinated solution but is not scalable due to the size of the search space.

Most research on the multi-manipulator object rearrangement problem has focused on developing efficient representations for the coupled approach. For example, the authors in [21] utilize a shared manipulator workspace to create a shared space graph, enabling reasoning about multi-robot cooperation and adapting a path planning heuristic for multi-manipulator tasks. Moreover, a series of studies [22]–[24] has focused on developing a concise object mode graph [15]. This graph captures valid transitions for pick, place, and hand-over actions and serves as a heuristic for guiding multi-modal motion planning [15]. Building on the work in [23], [25] utilizes the object-centric mode graph for multiple objects and applies multi-agent pathfinding techniques to generate non-conflicting sequences of object modes. For more complex assembly tasks, [26] employs a Mixed-Integer Linear Programming method for task assignment but did not effectively demonstrate scalability with respect to the number of robots, primarily due to the computational demands of roadmap generation and annotation processes.

Hybrid methods, such as [20], introduced a Conflict Based Search (CBS) variant to address the MR-TMP problem with multiply decomposable tasks. While this approach demonstrated the effectiveness of hybrid methods in complex multi-robot task and pathfinding problems, it has not been validated for higher-dimensional planning scenarios, such as multi-manipulator object rearrangement problems. DaSH [2],

a recent hybrid method, employs a hypergraph representation to concisely model hybrid robot state spaces and has been validated in the multi-manipulator object rearrangement problem. While it shows performance improvements—three orders of magnitude faster than the benchmark presented in [25]—its scalability is limited, particularly in scenarios with complex constraints. For example, in tasks requiring geometric constraints or multiple steps for completion, DaSH is limited in leveraging task-inferred constraint information during the query process. This limitation arises because a *combined* task and motion query in DaSH relies only on motion-collision constraints for replanning when the query fails, rather than incorporating task-specific constraints. In Section V, we demonstrate improved performance of Lazy-DaSH in environments with geometric constraints, even with a higher number of robots and objects.

III. PROBLEM DEFINITION

This section defines and explores the properties of the *task space*, defining key terminology related to the MR-TMP problem we address in this paper and its application to the multi-manipulator object rearrangement problem.

A. Task Space

In the MR-TMP framework [2], the *task space* \mathcal{T} is defined by three key components: the movable bodies \mathcal{B} , the configuration spaces \mathcal{W} , and the constraints \mathcal{C} . Each *task space element* $T_i = (B_i, W_i, C_i) \in \mathcal{T}$ consists of a subset of the movable bodies $B_i \subseteq \mathcal{B}$, its associated configuration space $W_i \subseteq \mathcal{W}$, and a set of constraints $C_i \subseteq \mathcal{C}$ that determine the validity of configurations within W_i . An MR-TMP problem has a set of *admissible* task space elements $\mathcal{T}^* \subseteq \mathcal{T}$, where the movable bodies and constraints of $T_i \in \mathcal{T}^*$ define a valid set of configurations for the entire system. The planner can consider *transitions* between sets of task space elements. These may reflect changes in the compositions of the subsets of moveable bodies and/or in the constraint sets included in elements.

B. Multi-manipulator Object Rearrangement Problem

In scenarios where manipulators are used to rearrange objects, the admissible task space elements $\mathcal{T}^* \subseteq \mathcal{T}_{\text{MANIP}}$ include robots, objects, and every possible combination of manipulator-object grasp pairs. These task space elements encompass not only the manipulators and objects themselves but also the manipulator-object pairs, along with their associated configuration spaces and constraints. For instance, task space elements for objects are characterized by the workspace's configuration space, constrained to ensure the object is on a stable surface. For manipulators, the elements are described by the robot's joint configuration space, with constraints to prevent self-collision. The elements for manipulator-object pairs are defined by the composite configuration space of both the robot and the object, constrained by the condition that the end-effector securely grasps the object.

Transitions are performed by pick, place, or hand-over actions. A pick action on an object, for example, removes

the constraint that the object is on a stable surface and adds a constraint that the object is in a stable grasp by the robot while changing the composition from independent elements, one with a robot and one with an object, to a coupled robot-object composition in the post-transition element. Transitions between task space elements are only possible at valid configurations between objects and robots for grasping. Consequently, a solution to this problem involves a discrete sequence of task space elements that specify which robot grasps which object, along with continuous motion paths within the configuration space of each task space element.

IV. THE LAZY-DASH METHOD

The overall structure of Lazy-DaSH is illustrated in Fig. 2. As in DaSH [2], we utilize a hierarchical representation structure, using hypergraph to represent the task spaces and motion spaces. As oppose to a standard graph, a (directed) hypergraph utilizes hyperedges (or hyperarcs) that connect multiple vertices simultaneously [27]. This is particularly useful for compactly encoding inter-robot interactions and constraints within a relatively small size compared to a standard graph [2].

In contrast to DaSH, Lazy-DaSH employs a two-stage hierarchical query approach: a *task query* within the task space hypergraph followed by a *motion query* within the motion hypergraph. This creates a strict hierarchical structure with a task planning layer and motion planning layer, where each layer has its corresponding representation construction phase and its query phase. The representation construction phase encodes the satisfaction of task and motion constraints between robots and objects, while the query phase sequences the constraint-satisfied task and motion.

Both Lazy-DaSH and DaSH perform hybrid and interleaved planning iterating between representation construction phases and query phases. However, they differ in their emphasis on sequencing and constraint satisfaction. DaSH prioritizes constraint satisfaction, as it pre-samples feasible configurations for each transition and generates feasible motions between each of these configurations before the query phase. Conversely, to identify the minimum constraints required, Lazy-DaSH prioritizes sequencing, as the task query phase first sequences high-level actions before addressing constraint satisfaction. The construction and query phases for both approaches are interleaved, with constraints being fed back whenever a feasible solution cannot be found.

The planning process of Lazy-DaSH starts by entering the *task planning layer*, first constructing the task space representation, or *task space hypergraph* ($\mathcal{H}_{\mathcal{T}}$), and subsequently generating a discrete task plan represented as *task-extended hypergraph* (\mathcal{H}_{TE}). The resulting task plan is an *unvalidated schedule* that presumes all motions within the task space elements are feasible and lazily validates motion feasibility in the subsequent motion planning layer. The *motion planning layer* first constructs the motion representation, or *motion hypergraph* ($\mathcal{H}_{\mathcal{M}}$), only for the task space elements identified as relevant by the task plan (unvalidated schedule). The motion feasibility is evaluated during the motion query phase

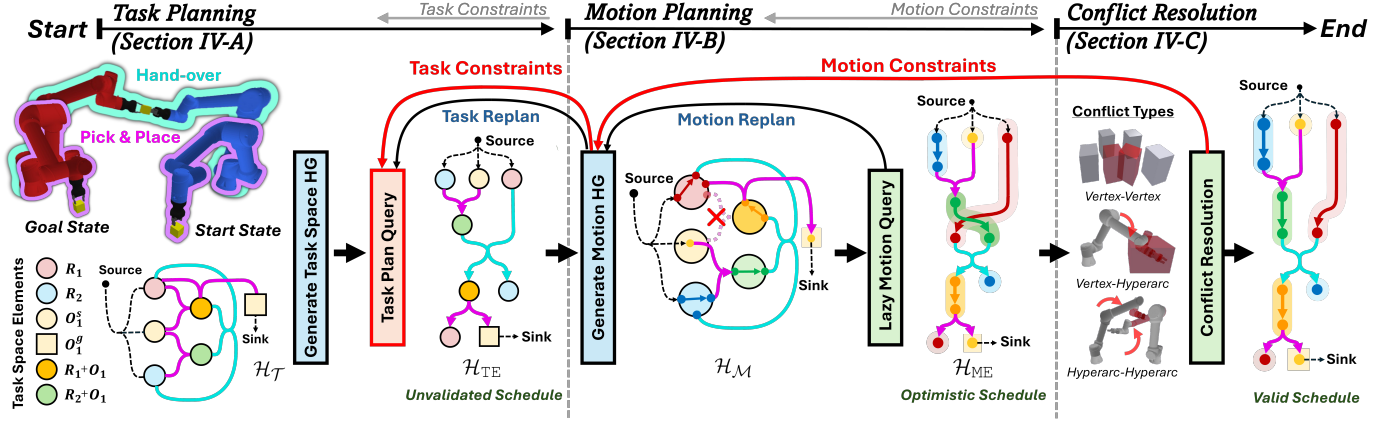


Fig. 2: Illustration of the hierarchical structure of the proposed Lazy-DaSH, showing two manipulators (R_1 and R_2) rearranging an object (O_1). The task query phase and the task constraint feedback scheme, which distinguish it from DaSH, are highlighted with red lines. This feature is also emphasized in Algorithm 1. Each layer of the hierarchy is detailed in corresponding sections.

Algorithm 1 Lazy-DaSH Approach.

Input: Initial task space element set T_{init} , goal task space element set T_{goal} , valid transition set A

Output: Motion plan S_M

```

1:  $S_T, S_M \leftarrow \emptyset$  ▷ task and motion schedules
2:  $C_T, C_M \leftarrow \emptyset$  ▷ task and motion constraints
3: while  $S_M$  not valid
4:   // Generate Task Space Hypergraph
5:    $\mathcal{H}_T \leftarrow \text{TASKSPACEHG}(\mathcal{H}_T, A)$ 
6:   // Query Unvalidated Schedule
7:    $S_T \leftarrow \text{QUERYTASKPLAN}(\mathcal{H}_T, C_T)$ 
8:   while  $S_T$  valid and  $S_M$  not valid
9:     // Generate Motion Hypergraph
10:     $\mathcal{H}_M, C_T, C_M \leftarrow \text{MOTIONHG}(S_T, \mathcal{H}_T, \mathcal{H}_M, C_M)$ 
11:    // Query Optimistic Schedule
12:     $S_M, C_T \leftarrow \text{QUERYMOTIONPLAN}(S_T, \mathcal{H}_T, \mathcal{H}_M, C_M)$ 
13:    if  $C_T \neq \emptyset$ 
14:      break
15:    // Generate Valid Schedule
16:     $S_M, C_M \leftarrow \text{RESOLVECONFLICTS}(S_M, C_M)$ 
17: return  $S_M$ 

```

by generating the *motion-extended hypergraph* (\mathcal{H}_{ME}). This approach alleviates the need for an unnecessarily expensive motion feasibility check for actions not included in the task plan or occurring after an action with no valid motion. The resulting motion plan is an *optimistic schedule*, requiring the *conflict resolution layer* to generate the collision-free *valid schedule*.

Lazy-DaSH adopts a *lazy* approach at three key stages within its hierarchical structure: first, during the task query phase, where it defers the motion feasibility check of the task sequence to the subsequent motion planning layer; and second, during the motion representation construction phase, where it assumes that motions are always feasible and postpones the feasibility check until the motion query phase; and lastly, during the conflict resolution layer where the lazy motion planning is used to replan the motion satisfying motion constraints.

The subsequent sections provide a detailed explanation of each layer in the hierarchy and a comprehensive comparison between the Lazy-DaSH and DaSH.

A. Task Planning Layer

The highest layer of the hierarchy, the task planning layer, encompasses the construction of the task representation and its query phases within the task-level domain.

1) *Representation Construction (Task Space Hypergraph)*: The task planning layer captures the most abstract level of representations through the task space hypergraph $\mathcal{H}_T = (\mathcal{V}_T, \mathcal{E}_T)$, where each task vertex $v_T = \langle T_i \rangle \in \mathcal{V}_T$ represents a task space element $T_i \in \mathcal{T}$, and task hyperarcs $E_T = \langle \text{Tail}, \text{Head} \rangle \in \mathcal{E}_T$ represent abstract transitions from the tail set comprising preconditions to the head set consisting of postconditions without explicit motion details.

For the multi-manipulator object rearrangement problems considered in this paper, the task vertices in \mathcal{H}_T representing the task space elements correspond to robots by themselves (R_1 and R_2 in Fig. 2), robots holding objects ($R_1 + O_1$ and $R_2 + O_1$), or objects at a particular location as indicated by the constraints in the task space element (O_s and O_g). The object-only task space elements in Lazy-DaSH differ from DaSH elements which are considered object-only task space elements with more general “stable surface” constraints. The location-specific constraints used for object-only task space elements in this work, for example, enable the start and goal constraints to be captured at the task space level (O_1^s and O_1^g in Fig. 2, respectively). This approach allows \mathcal{H}_T to be queried to generate a task plan (unvalidated schedule), linking the start object-only task space elements to the goal object-only task space elements.

Generating $\mathcal{H}_T = (\mathcal{V}_T, \mathcal{E}_T)$ begins by connecting the set of allowed task space elements (robots, objects with locations, and robots with objects) with all possible transitions. The objects with location task space elements include the start (and goal vertex) for each object, which are all connected with a single hyperarc to task source vertex v_T^{source} (and task sink vertex v_T^{sink}), to capture the full scope of the start (and goal) task states. The reachability of objects in the start and goal locations is then evaluated based on the robot’s capabilities (i.e., maximum payload and range) or grasp pose (i.e., a valid solution of inverse kinematics). However, the reachability only

indicates that the object is within the graspable range of some robots, without considering the motion feasibility of the robot reaching the object. Feasibility will be evaluated at the motion planning layer by running a motion planner.

The resulting $\mathcal{H}_{\mathcal{T}}$ provides a *queryable* task-level representation, encoding the abstract transitions between task space elements and reachability information for objects' start and goal states.

2) *Query (Task-extended Hypergraph)*: Since the hyperarcs in $\mathcal{H}_{\mathcal{T}}$ transition between different task space compositions, directly querying the task plan within $\mathcal{H}_{\mathcal{T}}$ may result in movable entities appearing in multiple task space compositions simultaneously. This may cause a task space element to perform multiple transitions at the same time, leading to an infeasible plan. To avoid this issue, we generate the task-extended hypergraph \mathcal{H}_{TE} , sequentially expanding the hyperarcs from the start task vertices by selectively choosing a viable transition for the frontiers in the current transition history.

The task-extended hypergraph is defined as $\mathcal{H}_{\text{TE}} = (\mathcal{V}_{\text{TE}}, \mathcal{E}_{\text{TE}})$. Each task-extended vertex $v_{\text{TE}} = \langle v_{\mathcal{T}}, \Pi_{v_{\text{TE}}^{\text{source}} v_{\text{TE}}} \rangle \in \mathcal{V}_{\text{TE}}$ is defined by a task vertex $v_{\mathcal{T}} \in \mathcal{V}_{\mathcal{T}}$ and a task-extended transition history $\Pi_{v_{\text{TE}}^{\text{source}} v_{\text{TE}}}$ that stores the history connecting from task-extended source vertex $v_{\text{TE}}^{\text{source}} = \langle v_{\mathcal{T}}^{\text{source}}, \emptyset \rangle$ to v_{TE} . Each task-extended hyperarc $E_{\text{TE}} = \langle \text{Tail}, \text{Head}, E_{\mathcal{T}} \rangle \in \mathcal{E}_{\text{TE}}$ includes the information about the tail, head, and task hyperarc that contributes to the history transitions. Beginning from $v_{\text{TE}}^{\text{source}}$, the search process finishes when the task-extended hyperarc finds the task-extended sink vertex $v_{\text{TE}}^{\text{sink}} = \langle v_{\mathcal{T}}^{\text{sink}}, \Pi_{v_{\text{TE}}^{\text{source}} v_{\text{TE}}^{\text{sink}}} \rangle$ in a head set. The task plan is obtained by extracting the task vertices $v_{\text{TE}.v_{\mathcal{T}}}$ from each v_{TE} along $\Pi_{v_{\text{TE}}^{\text{source}} v_{\text{TE}}^{\text{sink}}}$. The resulting task plan is an unvalidated schedule, which does not account for the motion feasibility along the task transitions.

As discussed in [2], three query strategies are available for hypergraph-based planning: Dijkstra-like, A*-like, and greedy hyperpath queries. In DaSH, the combined task and motion query explicitly computes motion costs, which are used to calculate admissible cost-to-go and hyperarc weights. This enables optimal solutions in both Dijkstra-like and A*-like hyperpath queries. By contrast, the greedy approach employs a heuristic to select the next hyperarc to add and backtracks if the selected actions fail to yield a feasible solution. It has been demonstrated that the greedy method achieves significantly faster and more scalable query performance while maintaining costs similar to those of optimal solutions and without compromising completeness [2].

In Lazy-DaSH, the task planning and motion planning layers are decoupled, requiring motion costs to be estimated rather than explicitly computed. This decoupled approach significantly reduces the computational effort required for representation generation, enabling faster and more scalable queries (Section V-D). Lazy-DaSH adopts a greedy search strategy guided by an estimated heuristic. For object rearrangement problems, an effective heuristic involves a distance-based approach: calculating the distance from the manipulator's base to the target object for grasping operations and the distance between the bases of two manipulators for handover

operations [25]. We then compute an estimated cost-to-go from each vertex based on $\mathcal{H}_{\mathcal{T}}$ and choose the action with the lowest estimated cost-to-go, backtracking when the actions are available.

B. Motion Planning Layer

This section describes the second layer of the hierarchy, the motion planning layer, which involves the construction of the motion representation and the query phases within the motion-level domain.

1) *Representation Construction (Motion Hypergraph)*: The motion hypergraph $\mathcal{H}_{\mathcal{M}} = (\mathcal{V}_{\mathcal{M}}, \mathcal{E}_{\mathcal{M}})$ captures the motion details of $\mathcal{H}_{\mathcal{T}}$. Each vertex $v_{\mathcal{M}} = \langle v_{\mathcal{T}}, q \rangle \in \mathcal{V}_{\mathcal{M}}$ contains both a task space vertex $v_{\mathcal{T}}$ and an explicit configuration q , and each motion hyperarc $E_{\mathcal{M}} = \langle \text{Tail}, \text{Head}, E_{\mathcal{T}}, \pi \rangle \in \mathcal{E}_{\mathcal{M}}$ consists of its tail and head sets, a corresponding task hyperarc $E_{\mathcal{T}}$, and a configuration path π connecting motion vertices $E_{\mathcal{M}}.\text{Tail}$ and $E_{\mathcal{M}}.\text{Head}$. As in DaSH [2], the motion hyperarcs can be categorized as a composite $E_{\mathcal{M}}^{\text{comp}}$, transition $E_{\mathcal{M}}^{\text{tran}}$, or move hyperarc $E_{\mathcal{M}}^{\text{move}}$. In the object rearrangement problem, for instance, a motion for merging or diverging of task space elements due to grasping or hand-over is a motion transition hyperarc $E_{\mathcal{M}}^{\text{tran}}$, and a motion of the manipulator or manipulator holding an object within the same task space elements is a motion move hyperarc $E_{\mathcal{M}}^{\text{move}}$.

The feasibility of each $E_{\mathcal{M}}$ reflects the feasibility of $E_{\mathcal{M}}.\pi$ and is validated in a lazy manner by querying a lazy sampling-based motion planner such as Lazy-PRM [5]. The edge-unvalidated roadmap generated by lazy sampling-based motion planners is validated in the order specified by the unvalidated schedule. If a motion query fails while tracing the unvalidated schedule, either a motion constraint is introduced or additional vertices are sampled to find an alternative path in the roadmap. The lazy motion validation approach minimizes unnecessary computational effort by deferring validation until it becomes necessary. If an invalid motion is found in the unvalidated schedule, it implies that the validity of the subsequent motions does not need to be checked yet as the task plan may change.

The construction of $\mathcal{H}_{\mathcal{M}}$ is similar to the motion hypergraph construction stage introduced in Section IV-C of [2], but our approach features a lazy motion validation during the construction. Initially, the transition sampler determines transition configurations (e.g., grasp and hand-over pose) only for transitions between the relevant task space elements. Then edge-unvalidated roadmaps are generated within the relevant task space elements to plan motion for $E_{\mathcal{M}}^{\text{tran}}$ and $E_{\mathcal{M}}^{\text{move}}$. If the transition sampler fails to generate valid transition configurations, the construction process stops and creates a task constraint to exclude the infeasible interaction during the replanning of the task plan.

2) *Query (Motion-extended Hypergraph)*: Similar to \mathcal{H}_{TE} , the motion sequence is queried by the motion-extended hypergraph \mathcal{H}_{ME} to avoid movable entities attempting multiple motions simultaneously. Since the abstract guideline of the motion plan is defined by the task plan, the motion-extended hypergraph is basically a motion-detailed version of the task plan. The feasibility of the motions between these transition

configurations is validated while tracing the task plan. If motion validation fails after a certain amount of effort (e.g., timeout), the task constraints are provided to the task query phase to enforce restrictions on the unsuccessful task sequence, prompting a replanning of the task plan.

The motion-extended hypergraph is defined as $\mathcal{H}_{\text{ME}} = (\mathcal{V}_{\text{ME}}, \mathcal{E}_{\text{ME}})$, similar to \mathcal{H}_{TE} but with motion information. Each motion-extended vertex $v_{\text{ME}} = \langle v_{\mathcal{M}}, \Pi_{v_{\text{ME}}^{\text{source}} v_{\text{ME}}} \rangle \in \mathcal{V}_{\text{ME}}$ consists of a motion vertex $v_{\mathcal{M}} \in \mathcal{V}_{\mathcal{M}}$ and a motion-extended transition history $\Pi_{v_{\text{ME}}^{\text{source}} v_{\text{ME}}}$ that stores a history extending from the motion-extended source vertex $v_{\text{ME}}^{\text{source}} = \langle v_{\mathcal{M}}, \emptyset \rangle$ to v_{ME} . Each motion-extended hyperarc $E_{\text{ME}} = \langle \text{Tail}, \text{Head}, E_{\mathcal{M}} \rangle \in \mathcal{E}_{\text{ME}}$ includes the information about the tail, head, and motion hyperarc that contributes to the history transitions. The motion query process begins at $v_{\text{ME}}^{\text{source}}$, expands the motion hyperarcs guided by the task plan, and terminates at $v_{\text{ME}}^{\text{sink}}$. The resulting motion history $\Pi_{v_{\text{ME}}^{\text{source}} v_{\text{ME}}^{\text{sink}}}$ in $v_{\text{ME}}^{\text{sink}}$ provides a motion plan that represents an optimistic schedule. This schedule ensures collision-free paths within each composition space but does not consider potential collisions with other moving bodies. The conflict resolution layer resolves these issues by refining individual motion plans to generate a collision-free schedule for all moving entities.

C. Conflict Resolution Layer

This section presents the final layer of the hierarchy, the conflict resolution layer, designed to identify motion conflicts between robots or objects that were not considered as coupled state spaces during the generation of the optimistic schedule. Any unsolvable motion conflicts lead to the creation of motion/task constraints, intended to enforce restrictions for replanning the motion/task plan.

1) *Conflicts*: There are three types of motion conflicts, arising from interactions between two motion vertices, two motion hyperarcs, or a motion vertex and a motion hyperarc. A *vertex-vertex* conflict occurs when two objects are in a colliding position and is often handled by resampling the object's positions within the planning area. A *hyperarc-hyperarc* conflict involves a collision between two moving entities and is generally resolved by adjusting the timing of the motion using a motion scheduling algorithm, or by replanning with path constraints to ensure the movable bodies avoid each other. A *hyperarc-vertex* conflict can arise when a static object obstructs the moving entity and is addressed by replanning the motion with constraints to navigate around the obstruction or by reordering the task sequence for colliding entities to pass through in a coordinated order. It is worth noticing that motion conflicts can be detected both in the motion query phase in the motion planning layer and the conflict resolution layer (Fig. 2).

2) *Constraint Feedback*: An overview of the constraint feedback is illustrated in Fig. 2. The hierarchical structure, comprising the task planning layer and the motion planning layer, enables the resolution of conflicts within these two distinct levels. The constraints are applied backward through the hierarchy. The motion conflicts are first addressed at the motion planning level by replanning the conflicting motions to find alternative motions. If these attempts consistently fail

(e.g., timeout), it is assumed that the current task plan cannot be executed with a feasible motion, leading to the generation of task constraints. These task constraints are designed to produce an alternative task sequence that seeks a feasible motion plan.

D. Discussion

As discussed at the beginning of Section IV, both Lazy-DaSH and DaSH can be categorized as hybrid and interleaved planning but differ in their emphasis on sequencing and constraint satisfaction, where DaSH prioritizes constraint satisfaction and Lazy-DaSH prioritizes sequencing. The approach for Lazy-DaSH aims to alleviate the exponential growth in representation size by identifying the minimum constraints required.

Comparing how DaSH and Lazy-DaSH manage their state space representations effectively illustrates the differences between the two approaches. From the perspective of the search process, the search space expands during the task/motion representation construction phases (blue arrows in Fig. 1) and is queried by the task/motion query phase (green and red arrows in Fig. 1). DaSH constructs the representations in two immediate sequential phases, exhaustively adding every feasible transition and motion for each robot, object, and their interactions into the representation. This approach leads to a continuous expansion of search space across the representation construction layers (blue arrows). Then the combined task and motion planning query phase finds a solution within the constructed representation (green arrows). Conversely, Lazy-DaSH in Fig. 1 scopes the search space by utilizing the task query phase (red arrows) immediately after constructing the task space representation (top blue arrows). This occurs before further expanding search space in the subsequent motion representation construction phase (bottom blue arrows). This approach results in a more compact search space compared to DaSH, containing only the essential information, which facilitates faster query processes.

V. VALIDATION

This section details the validation of Lazy-DaSH. We evaluated Lazy-DaSH across four scenarios, demonstrating its scalability and efficient constraint management across the hierarchical structure. Lazy-DaSH achieves a more compact representation and significantly faster total planning times, demonstrating superior scalability with twice the number of robots and objects. Notably, Lazy-DaSH improves planning times by an order of magnitude compared to DaSH [2], which itself has already outperformed the best existing method, Synchronized Multi-Arm Rearrangement (SMART) [25], by up to three orders of magnitude.

We begin by outlining the evaluation criteria, experiment scenarios, and method descriptions, followed by an analysis and discussion of the results. As part of the evaluation, we also demonstrate a hardware experiment for one of the scenarios as shown in Fig. 4.

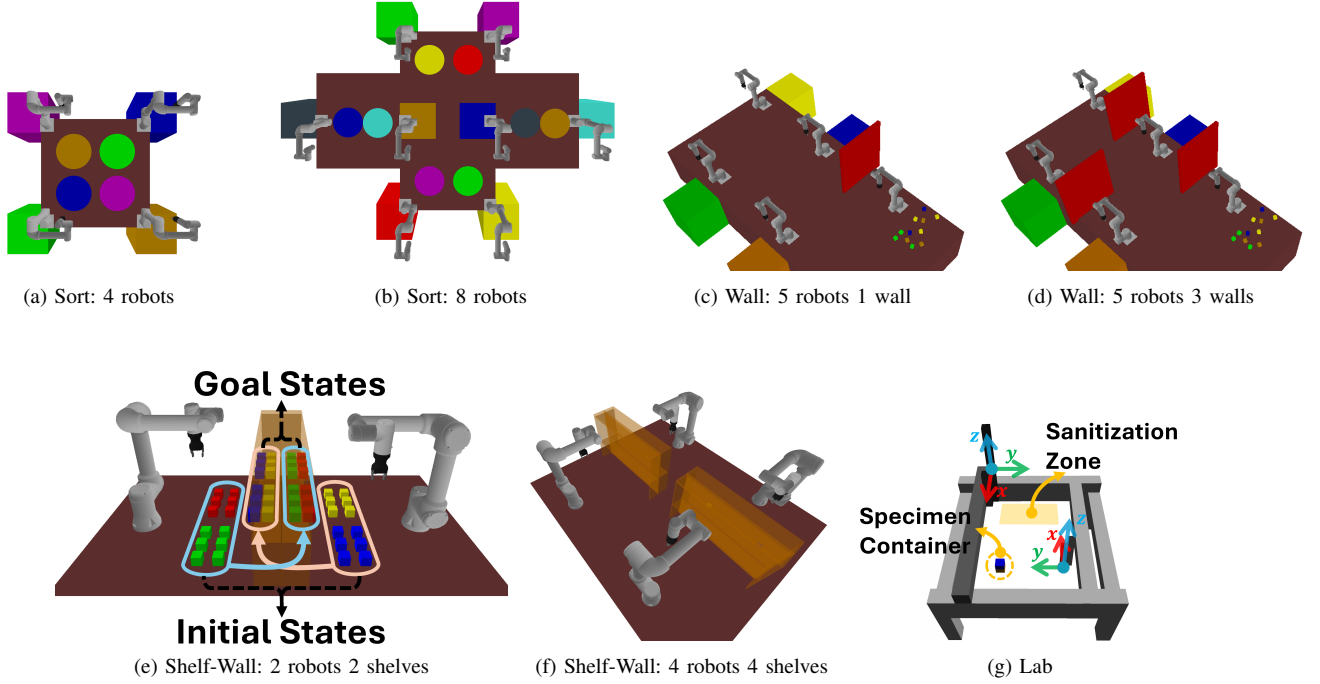


Fig. 3: Four different types of experiment scenarios. (a) and (b) show “Sort” scenarios where the initial clusters of objects are represented within colored circles, and each group must be moved to the matching square boxes. (c) and (d) represent “Wall” scenarios, featuring different numbers of walls. (e) and (f) illustrate the “Shelf-Wall” scenario, showing the start and goal locations of the blocks. Finally, (g) is the “Lab” scenario, involving 3-axis gantry robots along with descriptions of the problem entities.

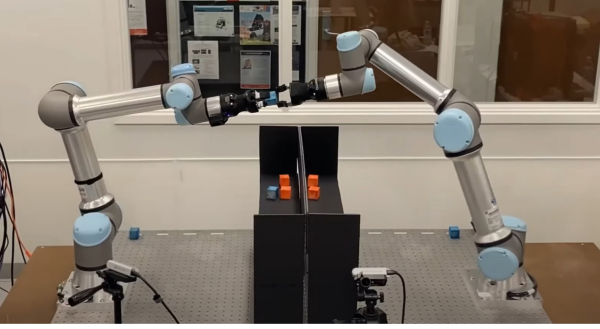


Fig. 4: A hardware experiment for the Shelf-Wall scenario. The top panels of the shelves have been removed for better visibility. A full video of demonstration can be found at: <https://youtu.be/bWQwy0dWAIJ>

A. Evaluation Criteria

As discussed in Section IV-D, Lazy-DaSH maintains a compact yet sufficient representation to ensure successful queries. This results in a smaller representation size compared to DaSH, leading to faster queries and improved scalability. To assess these advantages, we evaluate Lazy-DaSH in four distinct scenarios that highlight its capabilities, measuring representation size and overall planning time as the number of robots and objects increases, as shown in Figs. 5 and 6. A detailed analysis is discussed in Section V-D.

B. Method Descriptions

In this section, we provide implementation details of Lazy-DaSH and DaSH.

1) *DaSH*: Probabilistic Roadmap (PRM) [3] is used as a motion planner and motion feasibility is all validated during the \mathcal{H}_M construction phase. This validation eliminates the need for further motion validation during both the query phase and the conflict resolution phase. A variant of CBS-MP [28] is employed as a motion scheduler to sequence configurations over time in the conflict resolution layer.

2) *Lazy-DaSH*: Lazy-Probabilistic Roadmap (Lazy-PRM) [5] is used as the motion planner during the \mathcal{H}_M construction stage, with motion feasibility evaluated during the motion query and conflict resolution phases. The motion scheduler in the conflict resolution phase is identical to the one used in the DaSH method.

Both Lazy-DaSH and DaSH were implemented in C++ using the Parasol Planning Library. The experiments were conducted on a desktop computer equipped with an Intel Core i9-14900K CPU at 3.2 GHz and 64 GB of RAM.

C. Scenarios

Lazy-DaSH and DaSH are evaluated on the multi-manipulator object rearrangement problem, where manipulators are tasked to transport blocks from the start state to the goal state by performing grasp and hand-over actions. The cube-shaped blocks have randomly generated start and goal positions, ensuring that at least one robot can grasp them and transfer them to the goal.

We demonstrate four key capabilities: 1) efficient planning for large numbers of robots, 2) an effective constraint feedback mechanism for identifying infeasible robot interactions, 3)

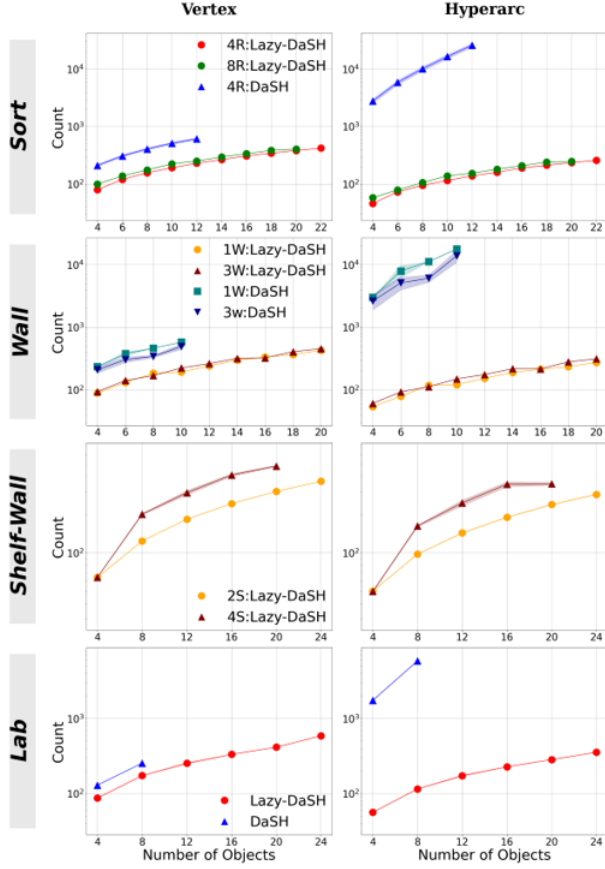


Fig. 5: Representation size comparison in terms of the number of vertex and hyperarc for Sort, Wall, Shelf-Wall, and Lab scenarios. The y-axis represents the number of vertex/hyperarc on a logarithmic scale, while the x-axis denotes the number of objects.

resolving geometric constraints, and 4) the ability to solve problems that require more than one step for task completion.

To evaluate these capabilities, we designed four scenarios: *Sort*, *Wall*, *Shelf-Wall*, and *Lab*, as illustrated in Fig. 3. In each scenario, we progressively increase task complexity by adding more robots, resulting in a greater number of interactions needed to transfer objects to their goal locations. Additionally, the number of objects gradually increases, further intensifying the task complexity. These increments expand the size of both the task space hypergraph and the motion hypergraph, significantly increasing the computational complexity of the query process.

All manipulators in the *Sort*, *Wall*, and *Shelf-Wall* scenarios are UR5e arms equipped with Hand-e grippers, and the *Lab* scenario uses gantry robots with customized end effectors tailored to task requirements. We demonstrate a hardware experiment for our *Shelf-Wall* scenario, which represents a more complex problem compared to the *Shelf* experiment demonstrated in DaSH [2]. The corresponding video is provided in the link shown in Fig. 4.

The tasks for each scenario are described below, along with their design objectives and a summary of the experimental results.

1) *Sort*: To assess Lazy-DaSH’s efficiency in large-scale planning, we designed Sort scenarios where four to sixteen

manipulators collaborate to transport colored objects to designated boxes as shown in Figs. 3a and 3b. This is essentially the same as the “cross sort” case described in DaSH paper [2], where objects must be delivered to the opposite side of the workstation. As the number of robots increases, this setup requires more complex coordination of task and motion, as each object must be handed over multiple times among the manipulators. It is important to note that the minimum number of required interaction grows as the number of robots increases for transferring each object to the goal location. The results show that Lazy-DaSH significantly improves scalability, successfully handling up to 8 robots with 20 objects, whereas DaSH could only handle up to 4 robots with 12 objects.

2) *Wall*: Lazy-DaSH makes assumptions on motion feasibility that may turn out to be incorrect. We evaluate the cost incurred by the method in recognizing and adapting to invalid motion assumptions, by introducing a set of thin walls to sorting problem, which violates the assumptions made in the lazy stages of the method. In *Wall*, illustrated in Figs. 3c and 3d, five manipulators are tasked with transferring the objects to designated boxes across the walls. Lazy-DaSH’s motion validation adopts an optimistic approach, which can result in infeasible motions being incorporated into the plan. To address this, the constraint feedback mechanism detects such infeasibility and triggers either a revised motion plan or necessary adjustments at the task planning level. To assess this capability, we progressively increase the number of walls, adding complexity to the problem. Manipulators near the wall are not only responsible for sorting the objects but also serve as intermediaries, assisting in passing the objects over the walls. The result shows that Lazy-DaSH scales more than twice as effectively as DaSH in terms of the number of objects in a presence of interaction obstructions.

3) *Shelf-Wall*: To demonstrate its ability to handle geometric constraints, DaSH [2] introduces the “Shelf” scenario, where objects must be placed on a shelf such that each rear object is completely blocked by the front object. We extend this concept with a more complex scenario, *Shelf-Wall*, which integrates the Shelf and Wall environments, treating each shelf as a barrier that obstructs both manipulator interactions and object access. As illustrated in Figs. 3e and 3f, two or four robots are tasked with rearrange objects while satisfying the geometric constraints. For example, green (yellow) blocks must be positioned behind the red (blue) blocks and placed on the shelf facing the opposite side. Manipulators must hand over objects to robots on the opposite side, as the shelves act as a physical wall between them. As the number of robots increases, each object transfer requires at least two handovers, similar to the Sort scenario.

Since these geometric constraints are not accounted for in the initial optimistic schedule, the conflict resolution layer detects them and ensures that subsequent queries generate a valid schedule that respects these constraints. Specifically, the conflict resolution layer identifies hyperarc-vertex conflicts, such as when a manipulator’s motion (hyperarc) attempts to pass through a statically placed object (vertex)—for example, a green (yellow) block intersecting a fixed red (blue) block. The results demonstrate that Lazy-DaSH successfully handles

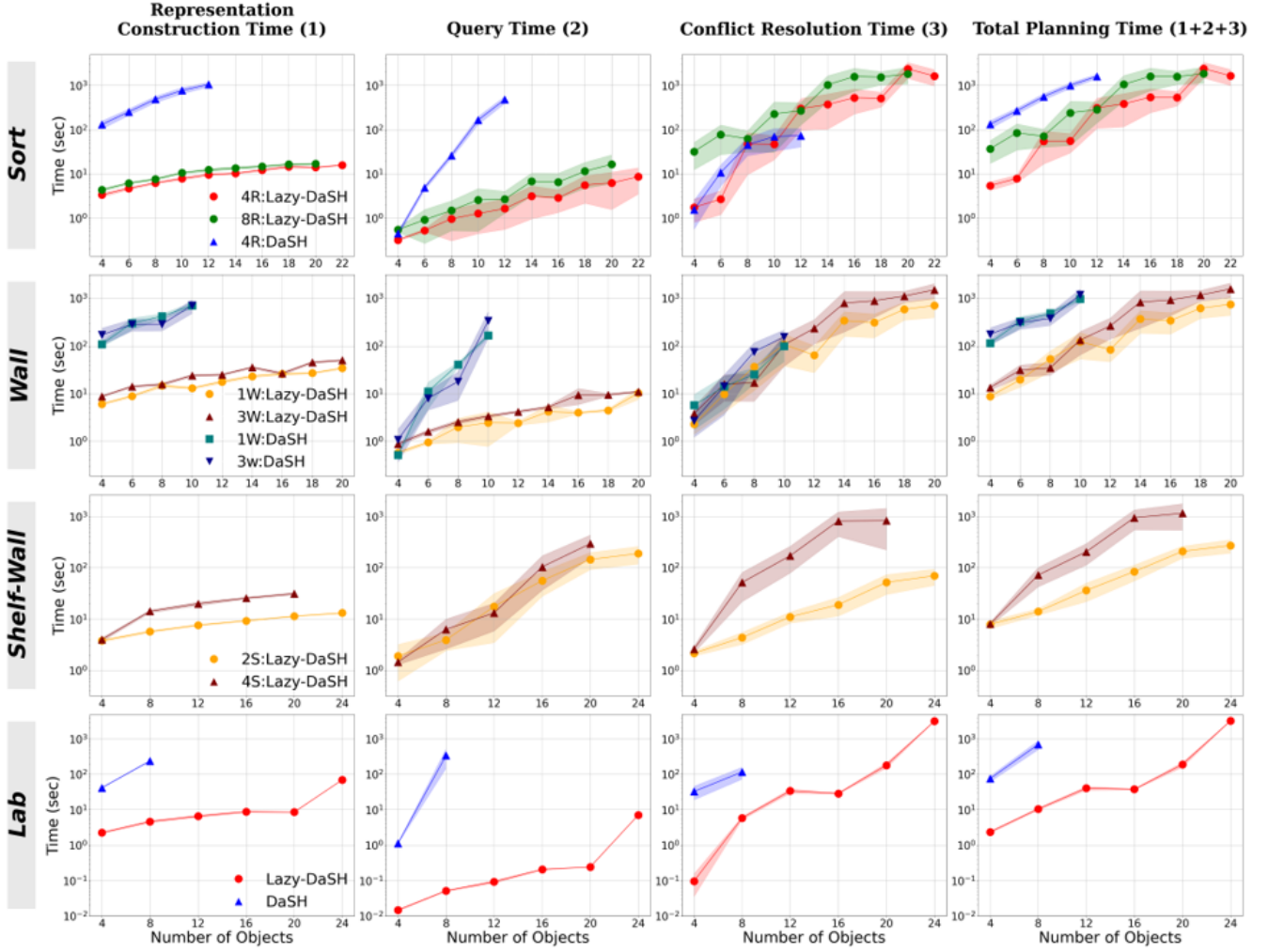


Fig. 6: A comparison of motion representation construction time (1), task and motion query time (2), conflict resolution time (3), and total planning time (1+2+3) is presented for the Sort, Wall, Shelf, and Lab scenarios. In DaSH, the query time reflects the combined task and motion planning time, whereas in Lazy-DaSH, the query time is the sum of the task query and motion query times. The y-axis represents planning time on a logarithmic scale and is kept consistent across each scenario to clearly compare the proportion of each time component (1, 2, and 3) in the total planning time (1+2+3).

4 robots with 20 objects, whereas DaSH fails to find a solution within the time limit even for a 2 robots scenario.

4) *Lab*: To address problems where each object requires multiple operations to reach its goal state, we introduce the Lab scenario, inspired by the Mind in Vitro (MiV) project [29]. In this scenario, two 3-axis gantry robots inspect specimens within a sealed container, as illustrated in Fig. 3g. The process begins with the robots removing the lid of the container and placing it in a predefined sanitization zone for sterilization. They then use tools attached to their end effectors to inspect the specimen. Once the inspection is complete, the lid is returned to the container to preserve the specimen's environment. Due to the limited space in the sanitization zone, the planner must determine a valid placement that prevents lid collisions. This placement is constrained by vertex-vertex conflicts, where each vertex represents a potential lid position in the sanitization zone. The results demonstrate that Lazy-DaSH outperforms DaSH, successfully handling more than twice the number of objects requiring multi-stage operations.

D. Analysis and Discussion

This section analyzes and discusses the experiment results, focusing on four distinct capabilities of Lazy-DaSH using the criteria defined in Section V-A.

1) *Overview*: Across all tested scenarios, Lazy-DaSH demonstrated significantly improved scalability compared to DaSH, as illustrated in Figures 5 and 6. The scalability analysis in [2] shows that the number of objects leads to linear growth in representation size, while the number of robots results in quadratic growth. This makes DaSH particularly inefficient in environments with many robots, where the exhaustive expansion of the search space imposes substantial computational overhead. This limitation was evident in the Sort scenarios, which are designed to test scalability with respect to the problem size in terms of both the number of robots and objects.

DaSH also struggles in scenarios that require frequent replanning at both the task and motion levels. In environments with complex constraints, such as Wall, Shelf-Wall, and Lab scenarios, DaSH fails to scale because it focused solely on

incorporating motion-level constraints without adapting the higher-level task structure. In particular, the Shelf-Wall scenario, which is heavily constrained by geometric constraints, was not solvable by DaSH even in its smallest environment setup. In contrast, Lazy-DaSH employs a hierarchical query framework that combines lazy motion validation with a constraint feedback mechanism. This design enables focused motion refinements, targeted backtracking, and high-level task replanning, thereby improving efficiency and scalability in complex environments.

2) *Representation Size*: The planning performance of both DaSH and Lazy-DaSH is directly influenced by the size of their representations, which serve as the foundation for iterative queries. We compare the size of $\mathcal{H}_{\mathcal{M}}$ in terms of the number of vertices and hyperarcs, as shown in Figure 5. The comparison of $\mathcal{H}_{\mathcal{T}}$ is omitted since Lazy-DaSH simply extends DaSH’s $\mathcal{H}_{\mathcal{T}}$ by incorporating additional object-only task space elements. The results show that the number of vertices and hyperarcs in $\mathcal{H}_{\mathcal{M}}$ is significantly smaller in Lazy-DaSH across all scenarios. Notably, the number of hyperarcs—critical due to their impact on motion validation checks—is up to two orders of magnitude smaller in Sort, Wall, and Lab, and up to one order of magnitude smaller in Shelf-Wall compared to DaSH. This reduction in representation size demonstrates the effectiveness of Lazy-DaSH’s task query phase in identifying only the necessary task space elements. Additionally, it highlights the efficacy of the constraint management system in selectively propagating only necessary constraints, ensuring a more compact and efficient representation. The impact of this reduction is further analyzed in the following discussion on overall planning performance.

3) *Planning Time*: Fig. 6 presents the total planning time along with a detailed breakdown. The first three columns represent the key components contributing to the total planning time: motion hypergraph construction, task and motion query, and conflict resolution. The fourth column shows the total planning time, which is the sum of these three components. To facilitate direct comparisons across different planning times, the y-axis for each scenario are kept consistent across all columns.

The representation construction time includes both task and motion representation construction, with motion representation accounting for the largest portion due to the computational cost of collision checking. In DaSH, this process involves constructing a fully validated roadmap upfront. In contrast, Lazy-DaSH adopts a lazy construction approach, initially generating an edge-invalidated roadmap and incrementally refining it in response to failures encountered during motion queries or conflict resolution. In addition to the reduced representation size in Lazy-DaSH, this incremental approach significantly decreases construction time, achieving up to two orders of magnitude reduction in scenarios where both methods are comparable.

The query times for DaSH and Lazy-DaSH differ in definition. In DaSH, it represents the combined task and motion planning query time, whereas in Lazy-DaSH, it is the sum of separate task and motion queries. In both methods, queries may be iteratively triggered by failures in planning or conflict

resolution, and the cumulative time for these iterations is reflected in the total query time. A key observation is that as the number of objects increases, the query time in DaSH grows at a much steeper rate compared to Lazy-DaSH. This is due to DaSH’s representation size becoming intractable, leading to an exponential increase in search space. In contrast, Lazy-DaSH maintains a more scalable query process, significantly reducing query time. The reduction reaches up to three orders of magnitude in scenarios where DaSH is able to find a solution.

Conflict resolution time, which involves the iterative detection and resolution of conflicts over entire motion paths, increasingly contributes to the total planning time as the number of objects grows. This is inherent to the conflict-based search approach [28], where motions are recomputed and entire paths are revalidated for collisions as conflicts are detected. As the length of the motion plan increases, typically due to an increased number of objects, the likelihood of recomputation and revalidation increases, becoming a primary source of computation in the overall planning process. Although this suggests that the conflict resolution layer could become a bottleneck in the planning process as the problem size increases, it is worth noting that this layer can be replaced with off the shelf schedulers or their variants to improve scalability. Future work will explore integrating alternative motion scheduling techniques into the conflict resolution layer to further enhance scalability.

VI. CONCLUSION

In this paper, we introduce **Lazy-Decomposable State Space Hypergraph (Lazy-DaSH)**, a novel hypergraph-based approach to multi-robot object rearrangement that extends DaSH. Lazy-DaSH separates task and motion planning into distinct layers connected through a constraint feedback mechanism and employs a lazy motion evaluation strategy, validating only the motions relevant to the candidate task plan to minimize unnecessary computation. The constraint feedback mechanism manages infeasible motions resulting from lazy evaluation and incorporates task/motion constraints detected by the conflict resolution layer, enabling dynamic updates and refinements to the planning representation.

This approach allows the planner to construct a minimal yet sufficient representation while efficiently managing constraints critical for task completion. Experimental results across four scenarios demonstrate that Lazy-DaSH significantly improves scalability and planning speed in highly constrained environments compared to DaSH. Additionally, one of the experiments is validated through hardware implementation: <https://youtu.be/bWQwy0dWAJI>. Code is available at: <https://github.com/parasollab/open-ppl/tree/lazy-hypergraph>

ACKNOWLEDGEMENT

This work was supported in part by the U.S. National Science Foundation’s “Expeditions: Mind in Vitro: Computing with Living Neurons” under award No. IIS-2123781, and by the IBM-Illinois Discovery Accelerator Institute and the Center for Networked Intelligent Components and Environments (C-NICE) at the University of Illinois.

Morales is supported in part by Asociación Mexicana de Cultura A.C.

REFERENCES

- [1] J. F. Canny, *The Complexity of Robot Motion Planning*. Cambridge, MA: MIT Press, 1988.
- [2] J. Motes, T. Chen, T. Bretl, M. M. Aguirre, and N. M. Amato, “Hypergraph-based multi-robot task and motion planning,” *IEEE Transactions on Robotics*, 2023.
- [3] L. E. Kavraki, P. Švestka, J. C. Latombe, and M. H. Overmars, “Probabilistic roadmaps for path planning in high-dimensional configuration spaces,” *IEEE Trans. Robot. Automat.*, vol. 12, no. 4, pp. 566–580, Aug. 1996.
- [4] S. M. Lavalle, “Rapidly-exploring random trees: A new tool for path planning,” Iowa State University, Tech. Rep. 11, 1998.
- [5] R. Bohlin and L. E. Kavraki, “Path planning using lazy prm,” in *Proc. IEEE Int. Conf. Robot. Autom. (ICRA)*, Apr. 2000.
- [6] L. Kavraki, M. Kolountzakis, and J.-C. Latombe, “Analysis of probabilistic roadmaps for path planning,” in *Proc. IEEE Int. Conf. Robot. Autom. (ICRA)*, vol. 4, 1996, pp. 3020–3025.
- [7] J. J. Kuffner and S. M. LaValle, “RRT-connect: An efficient approach to single-query path planning,” in *Proc. IEEE Int. Conf. Robot. Autom. (ICRA)*, 2000, pp. 995–1001.
- [8] A. Orthey, C. Chamzas, and L. E. Kavraki, “Sampling-based motion planning: A comparative review,” *Annual Review of Control, Robotics, and Autonomous Systems*, vol. 7, 2023.
- [9] C. R. Garrett, R. Chitnis, R. Holladay, B. Kim, T. Silver, L. P. Kaelbling, and T. Lozano-Pérez, “Integrated task and motion planning,” *Annual review of control, robotics, and autonomous systems*, vol. 4, pp. 265–293, 2021.
- [10] S. Srivastava, L. Riano, S. Russell, and P. Abbeel, “Using classical planners for tasks with continuous operators in robotics,” in *Workshops at the Twenty-Seventh AAAI Conference on Artificial Intelligence*, 2013.
- [11] C. R. Garrett, T. Lozano-Pérez, and L. P. Kaelbling, “Sampling-based methods for factored task and motion planning,” *The International Journal of Robotics Research*, vol. 37, no. 13-14, pp. 1796–1825, 2018.
- [12] —, “Pddlstream: Integrating symbolic planners and blackbox samplers via optimistic adaptive planning,” in *Proceedings of the international conference on automated planning and scheduling*, vol. 30, 2020, pp. 440–448.
- [13] A. Krontiris and K. E. Bekris, “Dealing with difficult instances of object rearrangement,” in *Robotics: Science and Systems*, vol. 1123, 2015.
- [14] C. R. Garrett, T. Lozano-Pérez, and L. P. Kaelbling, “Ffrob: An efficient heuristic for task and motion planning,” in *Algorithmic Foundations of Robotics XI: Selected Contributions of the Eleventh International Workshop on the Algorithmic Foundations of Robotics*. Springer, 2015, pp. 179–195.
- [15] K. Hauser and J.-C. Latombe, “Multi-modal motion planning in non-expansive spaces,” *Int. J. Robot. Res.*, vol. 29, no. 7, pp. 897–915, 2010.
- [16] J. Barry, L. P. Kaelbling, and T. Lozano-Pérez, “A hierarchical approach to manipulation with diverse actions,” in *2013 IEEE International Conference on Robotics and Automation*. IEEE, 2013, pp. 1799–1806.
- [17] W. Thomason and R. A. Knepper, “A unified sampling-based approach to integrated task and motion planning,” in *The International Symposium of Robotics Research*. Springer, 2019, pp. 773–788.
- [18] B. Kim, K. Lee, S. Lim, L. Kaelbling, and T. Lozano-Pérez, “Monte carlo tree search in continuous spaces using voronoi optimistic optimization with regret bounds,” in *Proceedings of the AAAI Conference on Artificial Intelligence*, vol. 34, no. 06, 2020, pp. 9916–9924.
- [19] B. Kim and L. Shimanuki, “Learning value functions with relational state representations for guiding task-and-motion planning,” in *Conference on robot learning*. PMLR, 2020, pp. 955–968.
- [20] J. Motes, R. Sandström, H. Lee, S. Thomas, and N. M. Amato, “Multi-robot task and motion planning with subtask dependencies,” *IEEE Robotics and Automation Letters*, vol. 5, no. 2, pp. 3338–3345, 2020.
- [21] K. Gao and J. Yu, “Toward efficient task planning for dual-arm tabletop object rearrangement,” in *2022 IEEE/RSJ International Conference on Intelligent Robots and Systems (IROS)*. IEEE, 2022, pp. 10 425–10 431.
- [22] A. Dobson and K. E. Bekris, “Planning representations and algorithms for prehensile multi-arm manipulation,” in *2015 IEEE/RSJ International Conference on Intelligent Robots and Systems (IROS)*. IEEE, 2015, pp. 6381–6386.
- [23] R. Shome and K. E. Bekris, “Anytime multi-arm task and motion planning for pick-and-place of individual objects via handoffs,” in *2019 International Symposium on Multi-Robot and Multi-Agent Systems (MRS)*. IEEE, 2019, pp. 37–43.
- [24] R. Shome, K. Solovey, A. Dobson, D. Halperin, and K. E. Bekris, “drrt*: Scalable and informed asymptotically-optimal multi-robot motion planning,” *Autonomous Robots*, vol. 44, no. 3, pp. 443–467, 2020.
- [25] R. Shome and K. E. Bekris, “Synchronized multi-arm rearrangement guided by mode graphs with capacity constraints,” in *International Workshop on the Algorithmic Foundations of Robotics*. Springer, 2020, pp. 243–260.
- [26] J. Chen, J. Li, Y. Huang, C. Garrett, D. Sun, C. Fan, A. Hofmann, C. Mueller, S. Koenig, and B. C. Williams, “Cooperative task and motion planning for multi-arm assembly systems,” *arXiv preprint arXiv:2203.02475*, 2022.
- [27] G. Gallo, G. Longo, S. Pallottino, and S. Nguyen, “Directed hypergraphs and applications,” *Discrete applied mathematics*, vol. 42, no. 2-3, pp. 177–201, 1993.
- [28] I. Solis, J. Motes, R. Sandström, and N. M. Amato, “Representation-optimal multi-robot motion planning using conflict-based search,” *IEEE Robotics and Automation Letters*, vol. 6, no. 3, pp. 4608–4615, 2021.
- [29] X. Zhang, Z. Dou, S. H. Kim, G. Upadhyay, D. Havert, S. Kang, K. Kazemi, K.-Y. Huang, O. Aydin, R. Huang, *et al.*, “Mind in vitro platforms: Versatile, scalable, robust, and open solutions to interfacing with living neurons,” *Advanced Science*, vol. 11, no. 11, p. 2306826, 2024.